SHS Web of Conferences **166**, 01071 (2023) https://doi.org/10.1051/shsconf/202316601071
EIMM 2022

Rapid reconstruction of sparse multiband signals based on MMV-SWACGP algorithm

Nan Yu*

Da Lian University, Da Lian 116622, China

Abstract. In this paper, an MMV-SWACGP algorithm is proposed, in order to solve the problem of pseudo-inverse computation in the iterative process of OMPMMV algorithm for multi-band signal reconstruction by compressed sensing. This algorithm reduces the complexity and computation of OMPMMV reconstruction algorithm. It is of great significance to the fast reconstruction of sparse multiband signals. Theoretical analysis and simulation results show that the proposed algorithm has faster computation speed and better noise stability.

1 Introduction

In recent years, Compressive Sensing (CS) has brought a revolutionary breakthrough for data acquisition technology. In this theoretical framework, the sampling rate is no longer determined by the signal bandwidth, but by the signal structure and effective information. Therefore, as long as the signal is sparse in a transformation domain, the effective information of the signal can be obtained at a rate much lower than the Nyquist sampling rate, and the analog signal can be digitized, and the signal can be reconstructed through the optimization algorithm, which has a broad application prospect[1-7].

In the compressed sensing theory, the OMPMMV algorithm used for multi-band signal reconstruction needs to carry out pseudo-inverse operation in each iteration process, which has a large computational complexity and amount of computation, and is difficult to implement in engineering[8-15].Therefore, the OMPMMV algorithm is transformed into an unconstrained optimization problem, and the MMV Stagewise Weak Adaptive Conjugate Gradient Pursuit algorithm is proposed.The algorithm adopts greedy selection method which is similar to OMPMMV algorithm, and replaces pseudo-inverse operation by gradient optimization to reduce the computational complexity and computation amount in signal reconstruction process.

This algorithm reduces the difficulty of the engineering implementation of signal reconstruction and provides a more feasible method for the engineering implementation of multi-band signal reconstruction. In this paper, through the reconstruction simulation of multi-band signals, it is verified that MMV-SWACGP algorithm can accurately reconstruct sparse multi-band signals, and maintain a high probability of signal reconstruction and good noise stability while having a faster operation speed.

* Corresponding author: yu19830116@163.com

2 Basic theory of compressed sensing

Let $\boldsymbol{X}$ be a finite length discrete time signal which can be viewed as a $N \times 1$ dimensional column vector of space $\boldsymbol{R}^N$. According to signal theory, any signal in $\boldsymbol{R}^N$ space can be represented by a linear combination of orthonormal basis vectors $\{\boldsymbol{\Psi}_i\}_{i=1}^N$. That is, any signal $\boldsymbol{X}$ can be expressed as

$$\boldsymbol{X} = \sum_{i=1}^{N} \alpha_i \boldsymbol{\psi}_i = \boldsymbol{\Psi\alpha}, \qquad i = 1, \cdots, N \tag{1}$$

where α is the column vector formed by the projection coefficient of the signal $\boldsymbol{X}$ on the $\boldsymbol{\Psi}$ domain. If the number of non-zero coefficients (or coefficients much larger than zero) of α is K, and K is much smaller than N, it indicates that the signal $\boldsymbol{X}$ is sparse or compressible in the domain $\boldsymbol{\Psi}$, and its sparsity is K.

In the theoretical framework of CS, the signal is no longer collected, but the observation matrix $\boldsymbol{\Phi}$ is used to project the signal $\boldsymbol{X}$ to the low-dimensional space for observation

$$\boldsymbol{Y} = \boldsymbol{\Phi X} = \boldsymbol{\Phi\Psi\alpha} \tag{2}$$

where, $\boldsymbol{Y}$ is the $M \times 1$ dimensional observation vector ($K < M$), and $\boldsymbol{\Phi}$ is the $M \times N$ dimensional observation matrix.

The main research contents of compressed sensing theory include:

Sparse representation: how to find the orthogonal basis $\boldsymbol{\Psi}$ so that the projection coefficient α of the signal is sparse;

Signal observation: how to design the observation matrix $\boldsymbol{\Phi}$ to ensure that the important information is not destroyed when the signal dimension is reduced;

Signal reconstruction: How to design reconstruction algorithms to reconstruct original signals $\boldsymbol{X}$ from observation vectors $\boldsymbol{Y}$ with high probability.

3 MMV- stagewise weak adaptive conjugate gradient pursuit

3.1 Mathematical model

In practical engineering, in many cases, the signals processed are multi-band signals, which contain multiple signal components. The support set of its Fourier transform is N disjoint frequency bands (the position of each frequency band is arbitrary and unknown), and the bandwidth of each frequency band does not exceed B, as shown in Figure 1.

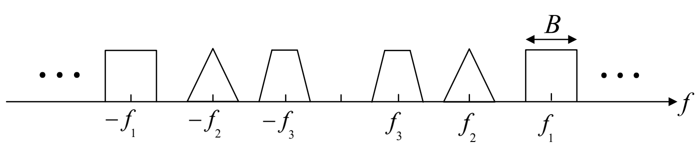

Fig. 1. Multiband signal model.

For compressed sensing acquisition and reconstruction of multiband signals, the sampling structure of Modulated Wideband Converter (MWC) was proposed[16-18], as shown in Figure 2. In this structure, the analog multi-band signals $x(t)$ enter N channels at the same time, and are multiplied by the mixing function $p_i(t)$ of each channel respectively. The $p_i(t)$ is an independent random function of Bernoulli distribution. After mixing, the signal passes through the low-pass filter with passband width of $1/T_s$. Then, low-rate sampling is realized through A/D with sampling frequency of $1/T_s$ to obtain compressed sensing data $y_i[n]$ of analog signals $x(t)$. Finally, the original signal is reconstructed by $y_i[n]$.

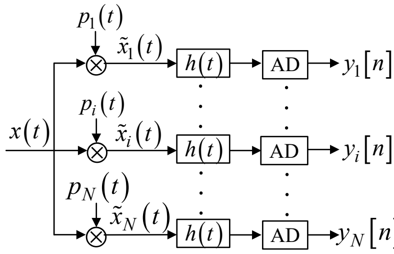

Fig. 2. Modulated wideband converter.

The output signal spectrum of MWC is shown in Figure 3, in which, c_{il} is the Fourier coefficient of the mixing function. The random sequence contains abundant frequency components, which can modulate all spectrum components within the monitoring bandwidth of the receiver to the baseband. The spectrum retained in the filter passband is a linear superposition of different spectrum components, which contains the complete information of the input signal. The output signal after low-pass filtering is sampled by Nyquist, and the observed value $y[n]$ contains each spectrum component of the input signal lossless, and the signal can be reconstructed from the baseband sampling value of multiple channels.

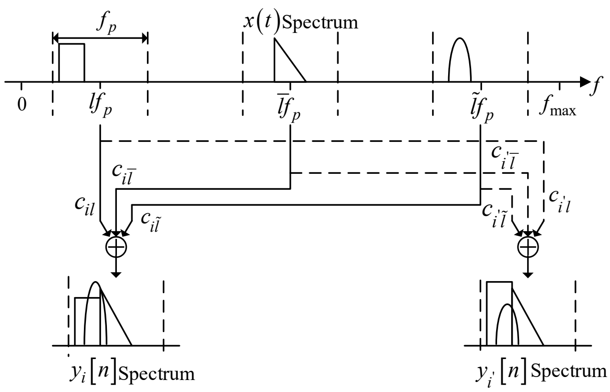

Fig. 3. The signal spectrum of MWC system.

3.2 Parameter selection

To analyze the relationship between sampling sequence $y[n]$ and unknown signal $x[n]$. First, define

$$\begin{aligned} f_p &= 1/T_p, \qquad F_p = \left[-f_p/2, +f_p/2\right] \\ f_s &= 1/T_s, \qquad F_s = \left[-f_s/2, +f_s/2\right] \end{aligned} \tag{3}$$

The Fourier expansion of $p_i(t)$ for the ith channel is

$$p_i(t) = \sum_{l=-\infty}^{\infty} c_{il} e^{j\frac{2\pi}{T_p}lt} \tag{4}$$

In which,

$$c_{il} = \frac{1}{T_p}\int_0^{T_p} e^{-j\frac{2\pi}{T_p}lt} dt \tag{5}$$

The Fourier transform of $\tilde{x}_i(t) = x_i(t)p_i(t)$ is

$$\tilde{X}_i(f) = \int_{-\infty}^{\infty} \tilde{x}_i(t)e^{-j2\pi ft}dt = \int_{-\infty}^{\infty} x(t)\left(\sum_{l=-\infty}^{\infty} c_{il}e^{j\frac{2\pi}{T_p}lt}\right)e^{-j2\pi ft}dt \tag{6}$$

$$= \sum_{l=-\infty}^{\infty} c_{il}\int_{-\infty}^{\infty} x(t)e^{-j2\pi\left(f-\frac{l}{T_p}\right)t}dt = \sum_{l=-\infty}^{\infty} c_{il}X\left(f - lf_p\right)$$

It can be seen that the spectrum of $\tilde{X}_i(f)$ is a linear combination of $X(f)$ translation f_p, and its spectrum is very wide. Therefore, a low-pass filter is needed to filter out the high-frequency component to meet the inherent bandwidth limit of A/D.

After passing through the low-pass filter with cutoff frequency $f_s/2$, the signal $\tilde{x}_i(t)$ is sampled by A/D with the sampling frequency of f_s, and the discrete value $y_i[n]$ is obtained, whose discrete Fourier transform is

$$Y_i\left(e^{j2\pi fT_s}\right) = \sum_{n=-\infty}^{\infty} y_i[n]e^{-j2\pi fnT_s} = \sum_{l=-L_0}^{+L_0} c_{il}X\left(f - lf_p\right), \qquad f \in f_s \tag{7}$$

Writing matrix form

$$\boldsymbol{Y}(f) = \mathbf{A}\boldsymbol{Z}(f), \quad f \in F_s \tag{8}$$

$$\boldsymbol{Z}(f) = \left[z_1(f), \cdots, z_L(f)\right]^{\mathrm{T}}, L = 2L_0 + 1 \tag{9}$$

$$z_i(f) = X\left(f + (i - L_0 - 1)f_p\right), \qquad 1 \le i \le L, f \in F_s \tag{10}$$

L_0 is the smallest integer that guarantees all the spectrum of $X(f)$ goes into $\boldsymbol{Y}(f)$

$$-\frac{f_s}{2} + (L_0 + 1)f_p \ge \frac{f_{NYQ}}{2} \to L_0 = \left\lceil \frac{f_{NYQ} + f_s}{2f_p} \right\rceil - 1 \tag{11}$$

$$L = 2L_0 + 1 \tag{12}$$

$\mathbf{A}$ is a matrix of coefficients c_{il}

$$\mathbf{A}_{il} = c_{i,-l} = c_{i,l}^{*}, \quad 1 \le i \le m \tag{13}$$

The relationship between $X(f)$ and $\boldsymbol{Z}(f)$ is shown in Figure 4. It can be seen from the figure that $\boldsymbol{Z}(f)$ is sparse, which meets the basic condition of CS -- sparsity.

The CS method can be used to reconstruct $\boldsymbol{Z}(f)$ through Equation (8), and then $X(f)$ can be obtained from Equation (10) to complete the collection and reconstruction of multi-frequency band signals.

According to the spectrum analysis results of the signals collected by MWC, the process of multi-band signal reconstruction can be regarded as the reconstruction of sparse spectrum $\boldsymbol{Z}(f)$ through $\boldsymbol{y}(f) = \boldsymbol{AZ}(f)$, and then the reconstruction of $X(f)$ through $\boldsymbol{Z}(f)$.

where, A is an $N \times L$ dimensional observation matrix composed of the Fourier coefficient c_{il} of the ith channel $p_i(t)$, and $\boldsymbol{Z}(f)$ is a matrix composed of the original spectrum $X(f)$ of the signal.

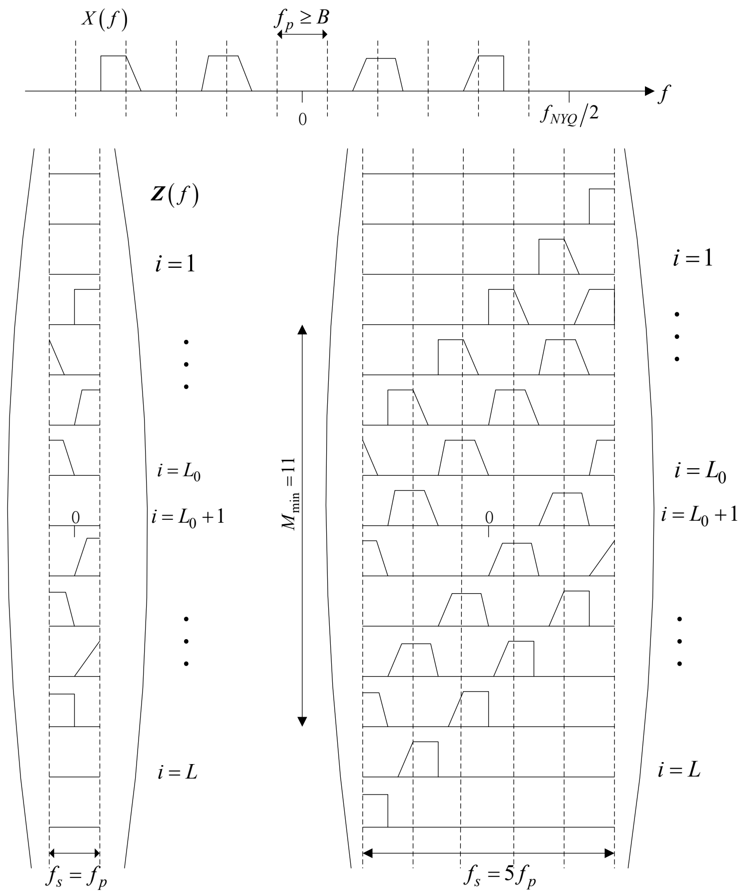

Fig. 4. The relationship of $X(f)$ and $\boldsymbol{Z}(f)$.

The signal reconstruction process starts with the construction of framework $\mathbf{V}$

$$\mathbf{Q} = \int_{f \in F_s} y(f) y^{\mathrm{H}}(f) df = \sum_{n=-\infty}^{+\infty} y[n] y^{\mathrm{T}}[n] \tag{14}$$

$$\mathbf{Q} = \mathbf{V}\mathbf{V}^{\mathrm{H}} \qquad \mathbf{V} = \mathbf{A}\mathbf{U} \tag{15}$$

Then find the support set S of the sparsest solution $\hat{\mathbf{U}}$ for $\mathbf{V} = \mathbf{A}\mathbf{U}$. Reconstruct $\boldsymbol{Z}(f)$ by the following formula

$$\boldsymbol{Z}_{\boldsymbol{S}}(f) = \mathbf{A}_{\boldsymbol{S}}^{\dagger} \boldsymbol{y}(f) \qquad z_i(f) = 0, \quad i \notin S \tag{16}$$

3.3 OMPMMV algorithm

Typical multi-band signal reconstruction algorithms include the orthogonal matching tracking algorithm (OMPMMV algorithm), which firstly defines the vector set, namely the set of column vectors corresponding to the non-zero row of the sparse matrix in the observation matrix, and the initial value is defined as the empty set.

The residual is initialized as $\mathbf{V}$. In each iteration, the residual is correlated with each column of the observation matrix $\mathbf{A}$ to obtain a set of correlation vectors. The norm of each correlation vector is calculated, and the column of matrix $\mathbf{A}$ corresponding to the maximum norm is put into the set of vectors.

The residuals are projected into the vector space spaned by the set of vectors, the solutions and residuals are updated, and the above iteration process is repeated until the iteration stop condition is satisfied. The OMPMMV algorithm flows as follows:

Input: observation matrix $\mathbf{A}$, observation vector $\mathbf{V}$;

Output: Support set $\boldsymbol{S}_t$;

Initialization: residuals $\mathbf{R}_0 = \mathbf{V}$, support sets $\boldsymbol{S}_0 = \varnothing$;

Repeat steps 1-5:

Step 1: Select the k th column of matrix $\mathbf{A}$, which satisfies $k = \arg\max_k \|\mathbf{X}_k\|_q$, where $\mathbf{X}_k = \mathbf{R}_{t-1}^{\mathrm{T}} \mathbf{A}_k$;

Step 2: Update the support set $\boldsymbol{S}_t = [\boldsymbol{S}_{t-1}, k]$, and record the reconstructed vector set $\mathbf{A}_{\boldsymbol{S}_t} = \left[\mathbf{A}_{\boldsymbol{S}_{t-1}}, \mathbf{A}_k\right]$;

Step 3: Estimate $\hat{\mathbf{U}}$, $\hat{\mathbf{U}}_t = \mathbf{A}_{\boldsymbol{S}_t}^{\dagger} \mathbf{V} = \left(\mathbf{A}_{\boldsymbol{S}_t}^{\mathrm{T}} \mathbf{A}_{\boldsymbol{S}_t}\right)^{-1} \mathbf{A}_{\boldsymbol{S}_t}^{\mathrm{T}} \mathbf{V}$;

Step 4: Update residuals $\mathbf{R}_t = \mathbf{V} - \mathbf{A}_{\boldsymbol{S}_t} \hat{\mathbf{U}}_t$, $t = t+1$;

Step 5: If the iteration stop condition is met, stop the iteration; If no, return to Step 1.

The selection of different vector norms in Step 1 has no great influence on the result. It only needs to meet $q \geq 1$, and $q = 2$ is generally chosen.

3.4 Improved algorithm

It can be seen from the process of OMPMMV algorithm that pseudo-inverse operation is required in each step of the iterative process, which is generally realized by QR decomposition or Cholesky decomposition. The main defect of the algorithm is that it has a large amount of computation and is difficult to meet the real-time requirements.

In order to improve the operation speed of OMPMMV-class algorithms, this paper proposed the MMV-gradient pursuit algorithm, and reduced the number of algorithm iterations according to the criteria selected by indexes. MMV-SWACGP algorithms is proposed.

3.4.1 MMV- gradient pursuit algorithm

The following equations need to be solved during each iteration of OMPMMV algorithm

$$\mathbf{V} = \mathbf{A}_{\boldsymbol{S}_t} \hat{\mathbf{U}}_t \tag{17}$$

Construct the objective function (different from the one constructed in solving the SMV problem) :

$$J\left(\hat{\mathbf{U}}_t\right) = \frac{1}{2} tr\left(\hat{\mathbf{U}}_t^{\mathrm{T}} \mathbf{A}_{\boldsymbol{S}_t}^{\mathrm{T}} \mathbf{A}_{\boldsymbol{S}_t} \hat{\mathbf{U}}_t\right) - tr\left(\mathbf{V}^{\mathrm{T}} \mathbf{A}_{\boldsymbol{S}_t} \hat{\mathbf{U}}_t\right) \xlongequal{\mathbf{B}_{\boldsymbol{S}_t} = \mathbf{A}_{\boldsymbol{S}_t}^{\mathrm{T}} \mathbf{A}_{\boldsymbol{S}_t}} \frac{1}{2} tr\left(\hat{\mathbf{U}}_t^{\mathrm{T}} \mathbf{B}_{\boldsymbol{S}_t} \hat{\mathbf{U}}_t\right) - tr\left(\mathbf{V}^{\mathrm{T}} \mathbf{A}_{\boldsymbol{S}_t} \hat{\mathbf{U}}_t\right) \tag{18}$$

where, $tr(\cdot)$ is the trace of the matrix. According to the condition of function minimization, the gradient of the objective function with respect to the vector $\hat{\mathbf{U}}_t$ should be equal to zero

$$\nabla_{\hat{\mathbf{U}}_t} J\left(\hat{\mathbf{U}}_t\right) = \mathbf{A}_{\boldsymbol{S}_t}^{\mathrm{T}} \left(\mathbf{A}_{\boldsymbol{S}_t} \hat{\mathbf{U}}_t - \mathbf{V}\right) = 0 \Rightarrow \mathbf{V} = \mathbf{A}_{\boldsymbol{S}_t} \hat{\mathbf{U}}_t \tag{19}$$

The above equation shows that the minimization of the objective function $J\left(\hat{\mathbf{U}}_t\right)$ has the same solution as the system of equations $\mathbf{V} = \mathbf{A}_{\boldsymbol{S}_t} \hat{\mathbf{U}}_t$.

Using the steepest descent method to find the minimum value of the objective function $J\left(\hat{\mathbf{U}}_t\right)$, the negative gradient of the objective function is

$$\mathbf{G}_{\boldsymbol{S}_t} = -\nabla_{\hat{\mathbf{U}}_t} J\left(\hat{\mathbf{U}}_t\right) = -\mathbf{A}_{\boldsymbol{S}_t}^{\mathrm{T}}\left(\mathbf{A}_{\boldsymbol{S}_t}\hat{\mathbf{U}}_t - \mathbf{V}\right) = \mathbf{A}_{\boldsymbol{S}_t}^{\mathrm{T}}\mathbf{R}_t \tag{20}$$

The solution in the t th iteration is

$$J\left(\hat{\mathbf{U}}_{t+1}\right) = J\left(\hat{\mathbf{U}}_t + \alpha_t \mathbf{G}_{\boldsymbol{S}_t}\right) = \min_{\alpha>0} J\left(\hat{\mathbf{U}}_t + \alpha \mathbf{G}_{\boldsymbol{S}_t}\right) \tag{21}$$

α_t is the step factor, whose function is to make the solution vector start from $\hat{\mathbf{U}}_t$ and find a better solution vector along the $\mathbf{G}_{\boldsymbol{S}_t}$ direction as the next iteration point, the requirement is

$$J\left(\hat{\mathbf{U}}_{t+1}\right) = J\left(\hat{\mathbf{U}}_t + \alpha_t \mathbf{G}_{\boldsymbol{S}_t}\right) = \min_{\alpha>0} J\left(\hat{\mathbf{U}}_t + \alpha \mathbf{G}_{\boldsymbol{S}_t}\right) \tag{22}$$

Making

$$\begin{aligned}\varphi(\alpha_t) &= J\left(\hat{\mathbf{U}}_{t-1} + \alpha_t \mathbf{G}_{\boldsymbol{S}_t}\right)\\ &= \frac{1}{2} tr\left[\left(\hat{\mathbf{U}}_{t-1} + \alpha_t \mathbf{G}_{\boldsymbol{S}_t}\right)^{\mathrm{T}} \mathbf{A}_{\boldsymbol{S}_t}^{\mathrm{T}}\mathbf{A}_{\boldsymbol{S}_t}\left(\hat{\mathbf{U}}_{t-1} + \alpha_t \mathbf{G}_{\boldsymbol{S}_t}\right)\right] - tr\left[\mathbf{V}^{\mathrm{T}}\mathbf{A}_{\boldsymbol{S}_t}\left(\hat{\mathbf{U}}_{t-1} + \alpha_t \mathbf{G}_{\boldsymbol{S}_t}\right)\right]\end{aligned} \tag{23}$$

To solve the optimal step is to find the α_t of $\varphi'(\alpha_t) = 0$

$$\begin{aligned}\varphi'(\alpha_t) &= \frac{1}{2} tr\left[\mathbf{G}_{\boldsymbol{S}_t}^{\mathrm{T}}\mathbf{A}_{\boldsymbol{S}_t}^{\mathrm{T}}\mathbf{A}_{\boldsymbol{S}_t}\hat{\mathbf{U}}_{t-1}\right] + \frac{1}{2} tr\left[\hat{\mathbf{U}}_{t-1}^{\mathrm{T}}\mathbf{A}_{\boldsymbol{S}_t}^{\mathrm{T}}\mathbf{A}_{\boldsymbol{S}_t}\mathbf{G}_{\boldsymbol{S}_t}\right] + \alpha_t \bullet tr\left[\mathbf{G}_{\boldsymbol{S}_t}^{\mathrm{T}}\mathbf{A}_{\boldsymbol{S}_t}^{\mathrm{T}}\mathbf{A}_{\boldsymbol{S}_t}\mathbf{G}_{\boldsymbol{S}_t}\right] - tr\left[\mathbf{V}^{\mathrm{T}}\mathbf{A}_{\boldsymbol{S}_t}\mathbf{G}_{\boldsymbol{S}_t}\right]\\ &= -tr\left[\mathbf{G}_{\boldsymbol{S}_t}^{\mathrm{T}}\mathbf{G}_{\boldsymbol{S}_t}\right] + \alpha_t \bullet tr\left[\mathbf{G}_{\boldsymbol{S}_t}^{\mathrm{T}}\mathbf{A}_{\boldsymbol{S}_t}^{\mathrm{T}}\mathbf{A}_{\boldsymbol{S}_t}\mathbf{G}_{\boldsymbol{S}_t}\right]\end{aligned} \tag{24}$$

$$\alpha_t = \frac{tr\left[\mathbf{G}_{\boldsymbol{S}_t}^{\mathrm{T}}\mathbf{G}_{\boldsymbol{S}_t}\right]}{tr\left[\mathbf{G}_{\boldsymbol{S}_t}^{\mathrm{T}}\mathbf{A}_{\boldsymbol{S}_t}^{\mathrm{T}}\mathbf{A}_{\boldsymbol{S}_t}\mathbf{G}_{\boldsymbol{S}_t}\right]} = \frac{tr\left[\left\langle \mathbf{R}_t, \mathbf{A}_{\boldsymbol{S}_t}\mathbf{G}_{\boldsymbol{S}_t}\right\rangle\right]}{tr\left[\left\langle \mathbf{A}_{\boldsymbol{S}_t}\mathbf{G}_{\boldsymbol{S}_t}, \mathbf{A}_{\boldsymbol{S}_t}\mathbf{G}_{\boldsymbol{S}_t}\right\rangle\right]} = \frac{tr\left[\left\langle \mathbf{R}_t, \mathbf{C}_t\right\rangle\right]}{tr\left[\left\langle \mathbf{C}_t, \mathbf{C}_t\right\rangle\right]} \tag{25}$$

In which $\mathbf{C}_t = \mathbf{A}_{\boldsymbol{S}_t}\mathbf{D}_{\boldsymbol{S}_t}$; $\mathbf{R}_t = \mathbf{V} - \mathbf{A}_{\boldsymbol{S}_t}\hat{\mathbf{U}}_t$ is the residual

3.4.2 MMV-conjugate gradient pursuit algorithm

In order to improve the convergence rate of MMV-Gradient Pursuit, this paper proposed an MMV-Conjugate gradient pursuit (MMV-CGP) algorithm. The algorithm uses the gradient descent method to update the iterative search direction of the jth sampling point, and is

$$\mathbf{D}_{\boldsymbol{S}_t}(:, j) = \mathbf{G}_{\boldsymbol{S}_t}(:, j) + b(j)\mathbf{D}_{\boldsymbol{S}_{t-1}}(:, j) \tag{26}$$

where, $\mathbf{D}_{\boldsymbol{S}_t}(:, j)$ is the iterative search direction of the jth sampling in this iteration; $\mathbf{G}_{\boldsymbol{S}_t}(:, j)$ is the gradient of the jth sampling in this iteration; $\mathbf{D}_{\boldsymbol{S}_{t-1}}(:, j)$ is the iterative search direction of the jth sampling in the last iteration.

In MMV-CGP algorithm, the search direction of each iteration and the search direction of the last iteration are conjugate relative to $\mathbf{B}_{\boldsymbol{S}_t}$, which is defined by conjugation

$$\mathbf{D}_{\boldsymbol{S}_t}^{\mathrm{H}}(:, j)\mathbf{B}_{\boldsymbol{S}_t}\mathbf{D}_{\boldsymbol{S}_k}(:, j) = 0, \qquad k = 1, \cdots, t-1 \tag{27}$$

where, $\mathbf{B}_{\boldsymbol{S}_t} = \mathbf{A}_{\boldsymbol{S}_t}^{\mathrm{T}}\mathbf{A}_{\boldsymbol{S}_t}$ is Hermitian positive definite matrix.

It's solved by conjugation

$$b(j) = -\frac{\mathbf{D}_{\boldsymbol{S}_{t-1}}^{\mathrm{T}}(:, j)\mathbf{B}_{\boldsymbol{S}_t}\mathbf{G}_{\boldsymbol{S}_t}(:, j)}{\mathbf{D}_{\boldsymbol{S}_{t-1}}^{\mathrm{T}}(:, j)\mathbf{B}_{\boldsymbol{S}_t}\mathbf{D}_{\boldsymbol{S}_{t-1}}(:, j)} = \frac{\left\langle\left(\mathbf{A}_{\boldsymbol{S}_t}\mathbf{D}_{\boldsymbol{S}_{t-1}}(:, j)\right), \left(\mathbf{A}_{\boldsymbol{S}_t}\mathbf{G}_{\boldsymbol{S}_t}(:, j)\right)\right\rangle}{\left\|\left(\mathbf{A}_{\boldsymbol{S}_t}\mathbf{D}_{\boldsymbol{S}_{t-1}}(:, j)\right)\right\|^2} \tag{28}$$

The solution in t th iteration is

$$\alpha_t = \frac{tr\left[\mathbf{D}_{S_t}^{\mathrm{T}}\mathbf{D}_{S_t}\right]}{tr\left[\mathbf{D}_{S_t}^{\mathrm{T}}\mathbf{A}_{S_t}^{\mathrm{T}}\mathbf{A}_{S_t}\mathbf{D}_{S_t}\right]} = \frac{tr\left[\left\langle \mathbf{R}_t, \mathbf{A}_{S_t}\mathbf{D}_{S_t}\right\rangle\right]}{tr\left[\left\langle \mathbf{A}_{S_t}\mathbf{D}_{S_t}, \mathbf{A}_{S_t}\mathbf{D}_{S_t}\right\rangle\right]} = \frac{tr\left[\left\langle \mathbf{R}_t, \mathbf{C}_t\right\rangle\right]}{tr\left[\left\langle \mathbf{C}_t, \mathbf{C}_t\right\rangle\right]} \tag{30}$$

In which $\mathbf{C}_t = \mathbf{A}_{S_t}\mathbf{D}_{S_t}$; $\mathbf{R}_t = \mathbf{V} - \mathbf{A}_{S_t}\hat{\mathbf{U}}_t$ is the residual.

3.4.3 MMV stagewise weak adaptive conjugate gradient pursuit algorithm

Similar to OMPMMV algorithm, MMV-conjugate gradient pursuit algorithm selects only one observation matrix column vector for sparse approximation in each iteration process, that is, MMV-conjugate gradient pursuit algorithm can also be improved through different selection criteria of support sets to reduce the number of iterations. By selecting three index selection criteria to improve MMV-CGP algorithm, MMV-RCGP, MMV-StCGP and MMV-SWCGP algorithms can be obtained.

In MMV-SWCGP algorithm, when β is fixed, the number of iterations increases or the support set is overestimated. Therefore, in this paper, MMV Stagewise Weak Adaptive Conjugate Gradient Pursuit (MMV-SWACGP) is proposed.

The algorithm adopts the conversion stage to gradually reduce β, divides each iteration into multiple stages, and determines the algorithm to enter the next stage or the next iteration by setting a threshold value. The initial value of β in each iteration process is the same.

Let ε_1 and ε_2 be thresholds for controlling iteration stop and stage conversion respectively. The specific steps of the algorithm are as follows:

Input: observation matrix $\mathbf{A}$, observation vector $\mathbf{V}$;

Output: Support set $\boldsymbol{S}_t$;

Initialization: residuals $\mathbf{R}_0 = \mathbf{V}$, weakening parameters $\beta_{start} \in [0.9,1)$, stage steps $step \in [0.5,1]$, support sets $\boldsymbol{S}_0 = \varnothing$, iteration counters $t = 1$;

Determine whether to stop the iteration. If $\|\mathbf{R}\|_2 / \|\mathbf{V}\|_2 \le \varepsilon_1$, the iteration will stop and the signal will be output. Otherwise, the iteration cycle will be performed in steps 1-5;

Step 1: Calculate the ℓ_2 -norm of the correlation coefficients $\boldsymbol{\mu} = \left\{\mu_i \middle| \mu_i = \left\|\langle \mathbf{R}, A_i\rangle\right\|_2, i = 1,2,\cdots,L\right\}$;

Step 2: Calculate the threshold $h_{\text{MMV-SWACGP}} = \beta \left\|\left\|\langle \mathbf{R}, A_i\rangle\right\|_2\right\|_\infty = \beta \max_i |\mu_i|$ and update the index set $\boldsymbol{S}_t = \boldsymbol{S}_{t-1} \cup \left\{i : |\mu_i| \ge h_{\text{MMV-SWACGP}}\right\}$;

Step 3: (1) Calculate the gradient $\mathbf{G}_{S_t} = \mathbf{A}_{S_t}^{\mathrm{T}}\mathbf{R}_{t-1}$

If $t = 1$

$\mathbf{D}_{S_t} = \mathbf{G}_{S_t}$

$\mathbf{V}_t = \mathbf{A}_{S_t}\mathbf{D}_{S_t}$

Otherwise

$\mathbf{W}_t = \mathbf{A}_{S_t}\mathbf{G}_{S_t}$

$\mathbf{C}_t(:,j) = \text{-}\mathbf{V}_{t-1}'(:,j)\mathbf{W}_t(:,j) / \eta_{t-1}(j,j)$

$\mathbf{V}_t(:,j) = \mathbf{W}_t(:,j) + \mathbf{C}_t(:,j)\mathbf{V}_{t-1}(:,j)$

(2) $\eta_t = \langle \mathbf{V}_t, \mathbf{V}_t\rangle$

(3) $\alpha_t = tr\left(\langle \mathbf{R}_{t-1}, \mathbf{V}_t\rangle\right) / tr(\mathbf{Z})$

Step 4: Update residuals $\mathbf{R}_t = \mathbf{R}_{t-1} - \alpha_t \mathbf{V}_t$;

Step 5: If the conditions for stopping iteration are met, stop iteration; if not, determine whether β_t needs to be adjusted; if $\|\mathbf{R}_t\|_2 / \|\mathbf{R}_{t-1}\|_2 \le \varepsilon_2$, set $\beta_t = \beta_t - step$, return to Step 1; Otherwise, set $t = t+1$ and $\beta_{t+1} = \beta_{start}$, proceed to the next iteration.

Output signal

$$\boldsymbol{z}_{\boldsymbol{S}}(f) = \mathbf{A}_{\boldsymbol{S}}^{\dagger} \boldsymbol{y}(f) \qquad z_i(f) = 0, \quad i \notin S \tag{31}$$

4 Simulation analysis

4.1 Simulation signal

The mathematical expression of linear frequency modulation (LFM) signal is:

$$x(t) = A\exp\left[j2\pi \left(\frac{1}{2}kt^2 + f_c t \right) \right] \tag{32}$$

where f_c is the initial signal frequency, k is the frequency modulation slope, and A is the amplitude.

LFM signals are sparse in the frequency domain, and multiple signals can constitute sparse multi-band signals, which can be reconstructed by using CS algorithm. The experiment in this paper contains 6 narrow-band LFM signals, whose composition is shown in Table 1. The pulse width is 6us, and the spectrum is shown in Figure 5 (the lower band of each frequency band in the figure is the initial signal frequency, and the upper band is the initial frequency plus signal bandwidth). Multiple narrow-band LFM signals constitute sparse multi-band signals.

Table 1. The signal component.

	signal 1	signal 2	signal 3	signal 4	signal 5	signal 6
Amplitude	0.9	1	0.8	0.6	0.4	0.7
Initial frequency (f /MHZ)	60	140	220	300	380	460
Bandwidth(f /MHZ)	50	25	25	40	30	40
Frequency modulation slope(k /10^{12})	8.3333	4.1667	4.1667	6.6667	5.0000	6.6667

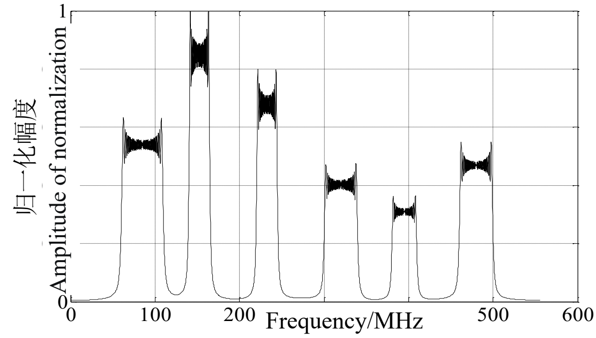

Fig. 5. Sparse multiband LFM signal.

4.2 Simulation experiment

In the experiment, OMPMMV algorithm and MMV-SWACGP algorithm were respectively used to reconstruct one-dimensional multi-band LFM signal (sampling rate is 51.282MHz), and the performance of the algorithm was compared and analyzed.

Experiment 1: In the noiseless environment

1) Verify the feasibility of multi-band signal reconstruction by MMV-SWACGP algorithm, and the reconstructed spectrum is depicted in Figure 6;

2) The signal was reconstructed through 12 iterations. The average CPU running time of each iteration of the algorithm was shown in Table 2. The reconstruction errors were 1.08% and 1.19%, respectively.

Experiment 2: In the environment containing additive white noise

1) Change the signal-to-noise ratio, run Monte Carlo simulation for 1000 times for the two algorithms, and count the reconstruction probability of the algorithm under different signal-to-noise ratios. The result curve is depicted in Figure 7.

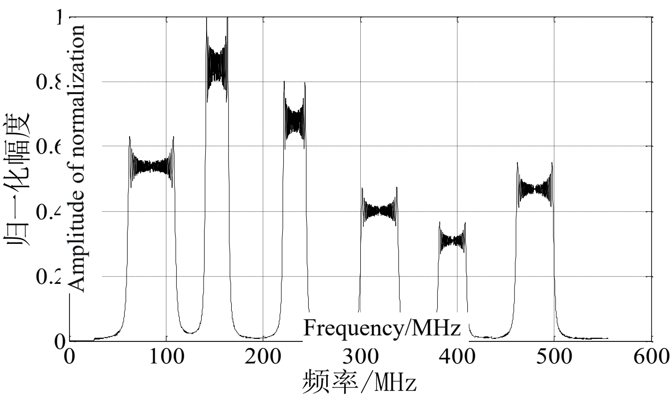

Fig 6. The multiband signal reconstruction spectrum of MMV-SWACGP algorithm.

Table 2. The average CPU operation time per iteration of the algorithm.

algorithm Number of iterations	first	second	third	fourth	fifth	sixth	seventh
OMPMMV(t/ms)	1.913	2.088	2.146	2.155	2.202	2.215	2.235
MMV-SWACGP(t/ms)	1.430	2.273	1.899	1.861	1.849	1.864	1.861

algorithm Number of iterations	eighth	ninth	tenth	eleventh	twelfth	Total time
OMPMMV(t/ms)	2.445	2.653	2.701	3.086	4.072	30.1
MMV-SWACGP(t/ms)	2.141	1.915	1.902	1.896	1.918	23.1

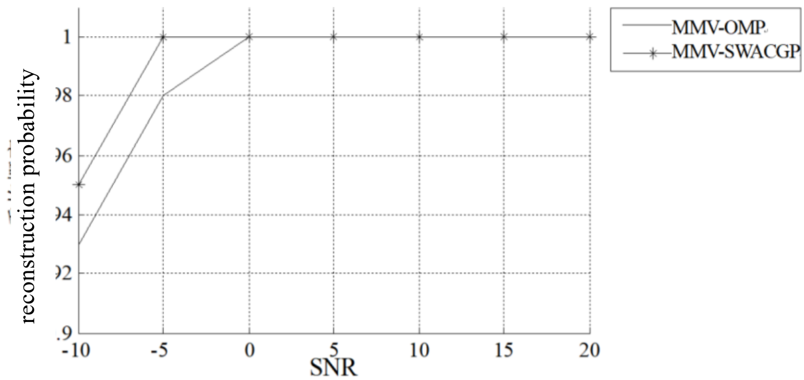

Fig. 7. The reconstruction probability on different SNR.

4.3 Simulation analysis

Based on the simulation results, the following conclusions can be drawn:

By comparing Figure 7 and Figure 6, it can be seen that the MMV-SWACGP algorithm proposed in this paper can accurately reconstruct multi-band signals;

Table 2 shows that the CPU running time of MMV-SWACGP algorithm is 76.7% of that of OMPMMV algorithm. In the two algorithms, as the number of iterations increases, the dimension of $\mathbf{A}_{S_t}$ increases, resulting in the OMPMMV algorithm iteration process, the solution of the pseudo-inverse operation of the complexity and operation time increased significantly. However, MMV-SWACGP algorithm does not require pseudo-inverse operation, and the dimension increase of $\mathbf{A}_{S_t}$ does not significantly increase the operation complexity. Therefore, the CPU running time of MMV-SWACGP algorithm is lower than that of OMPMMV algorithm.

As can be seen from Figure 8, both MMV-SWACGP algorithm and OMPMMV algorithm have good noise stability. When the SNR drops to -10dB, the reconstruction probability is still higher than 90%. In the two algorithms, the decrease of SNR has no significant effect on the reconstruction of signal support set. Therefore, both algorithms have good noise stability for the reconstruction of the original signal.

In conclusion, compared with OMPMMV algorithm, MMV-SWACGP algorithm can not only ensure the reconstruction accuracy and good noise stability, but also reduce the CPU running time of signal reconstruction. When the number of signals increases, the time decreases more significantly.

5 The conclusion

When CS theory is used to solve the reconstruction of multi-band signal, OMPMMV algorithm has the problems of engineering complexity and large amount of computation.

In this paper, a new algorithm is proposed, which transforms OMPMMV algorithm into unconstrained optimization problem, and MMV-SWACGP algorithm is proposed based on conjugate gradient principle. Theoretical analysis shows that this algorithm does not need pseudo-inverse operation, can reduce the complexity of signal reconstruction and the amount of calculation, and is easy to engineering implementation, more suitable for the application of high real-time requirements.In this paper, the simulation verifies that the algorithm can accurately reconstruct sparse multi-band signals, and the results show that the algorithm has faster operation speed while maintaining high reconstruction probability

 https://doi.org/10.1051/shsconf/202316601071

and good noise stability, which provides a more feasible algorithm for the engineering realization of multi-band signal reconstruction.

References

1. Donoho D L. Compressed sensing. Information Theory, IEEE Transactions on, **52**, 4 (2006).
2. Keying W, Xiaoyong G. Compressive sensing of digital sparse signals. Wireless Communications and Networking Conference (WCNC), (2011).
3. Qaisar, S., Bilal, R.M., Iqbal, W., et al. Compressive sensing: From theory to applications, a survey. Communications and Networks, Journal of, **15**, 5 (2013).
4. Candes, E., Becker, S. Compressive sensing: Principles and hardware implementations. ESSCIRC (ESSCIRC), 2013 Proceedings of the, (2013).
5. Qi-Fan Yang, Ke Fang, Yong-Jun Xie. Research on the Relation between the Number of Measurements and Signal Sparsity in Compressed Sensing. 2018 IEEE 3rd Advanced Information Technology, Electronic and Automation Control Conference (IAEAC), (2018).
6. Yuchen Shi, Pingyi Fan, Zheqi Zhu, et al. MIM-CS: Message Importance Measure for Compressed Sensing. 2021 IEEE International Mediterranean Conference on Communications and Networking (MeditCom), (2021).
7. Jiaqi Sun;Wenrui Dai, Chenglin Li, Junni Zou, et al. Compressive Sensing via Unfolded ℓ0-constrained Convolutional Sparse Coding. 2021 Data Compression Conference (DCC), (2021).
8. van den Berg E, Friedlander M P. Theoretical and Empirical Results for Recovery From Multiple Measurements. Information Theory, IEEE Transactions on, **56**, 5 (2010).
9. Blanchard, J.D., Cermak, M., Hanle, D., et al.. Greedy Algorithms for Joint Sparse Recovery. Signal Processing, IEEE Transactions on, **62**, 7 (2014)
10. Deepa, K G, Ambat, Sooraj K., Hari, K.V.S.. Modified greedy pursuits for improving sparse recovery. Communications (NCC), 2014 Twentieth National Conference on, (2014).
11. Mishali M, Eldar Y C. Blind Multiband Signal Reconstruction: Compressed Sensing for Analog Signals. Signal Processing, IEEE Transactions on, **57**, 3 (2009).
12. Majumdar A, Ward R K, Aboulnasr T. Algorithms to Approximately Solve NP Hard Row-Sparse MMV Recovery Problem: Application to Compressive Color Imaging. Emerging and Selected Topics in Circuits and Systems, IEEE Journal on, **2**, 3 (2012).
13. Xinquan Gao, Xuewei Wang, Jinglin Zhou. A Robust Orthogonal Matching Pursuit Based on L1 Norm. 2020 Chinese Control And Decision Conference (CCDC), (2020).
14. Blumensath T, Davies M E. Gradient Pursuits. Signal Processing, IEEE Transactions on, **56**, 6 (2008).
15. Blumensath T, Davies M E. Stagewise Weak Gradient Pursuits. Signal Processing, IEEE Transactions on, **57**, 11 (2009).
16. Iliadis, M., Watt, J., Spinoulas, L., et al. Video compressive sensing using multiple measurement vectors. Image Processing (ICIP), 2013 20th IEEE International Conference on, (2013).

17. Mishali M, Eldar Y C. From Theory to Practice: Sub-Nyquist Sampling of Sparse Wideband Analog Signals. Selected Topics in Signal Processing, IEEE Journal of, **4**, 2 (2010).
18. Hassan Mortada, Olivier Rabaste, Jonathan Bosse. Structured dictionary optimization: application to the modulated wideband converter. 2019 IEEE 8th International Workshop on Computational Advances in Multi-Sensor Adaptive Processing (CAMSAP), (2019).